



## **CAMPBELL-BOZORGNIA NEXT GENERATION ATTENUATION (NGA) RELATIONS FOR PGA, PGV AND SPECTRAL ACCELERATION: A PROGRESS REPORT**

K. W. Campbell<sup>1</sup> and Y. Bozorgnia<sup>2</sup>

### **ABSTRACT**

The authors are one of five teams developing empirical ground motion (attenuation) relations for active shallow crustal regions as part of the PEER Next Generation Attenuation (NGA) Project. Each Developer Team was provided with a common database of worldwide strong-motion recordings and supporting metadata, but was given the freedom to use separate data selection criteria, parameters, functional forms, and statistical regression methods. We chose to exclude aftershocks and poorly recorded earthquakes using criteria that required smaller events to have a larger number of recordings than larger events. One of the biggest challenges was to develop a functional form that accounted for the apparent change in magnitude scaling around  $M$  6.5–7.0 as suggested from several recent large earthquakes in Alaska, California, Turkey, and Taiwan. After extensive exploratory analysis, we selected a trilinear rather than the more traditional quadratic functional form to model the magnitude-scaling characteristics of ground motion. Parameters included in the model are moment magnitude, closest distance to rupture and to the surface projection of rupture, buried reverse faulting, normal faulting, sediment depth (both shallow and basin effects), hanging-wall effects, average shear-wave velocity in the top 30 m, and nonlinear soil behavior as a function of shear-wave velocity and rock PGA.

### **Introduction**

In 2003, we and four other Developer Teams were selected to participate in a Pacific Earthquake Engineering Research (PEER) Center project to empirically develop Next Generation Attenuation (NGA) relations. Each Team used a common worldwide database of strong-motion recordings and supporting metadata that was developed by a sixth NGA team, but each Team was allowed to apply its own selection criteria regarding which earthquakes, recordings, functional forms, and independent variables to use in developing its model. The NGA Project specified a set of minimum requirements that all models should meet, the most notable of which were that ground-motion predictions should be valid to  $M$  8.5 for strike-slip earthquakes, to  $M$  8.0 for reverse earthquakes, to distances of 200 km, and to periods of 10 sec. A thorough description of the database development and project requirements are provided in

---

<sup>1</sup>Vice President, EQECAT, Inc., Beaverton, OR 97006

<sup>2</sup>Associate Director, PEER, University of California, Berkeley, CA 94720

several companion papers in this volume.

At the time this paper was written, our model had not yet been finalized. As a result, this paper should be considered a progress report. The functional forms are not likely to change significantly, but there are a few issues yet to be resolved that could require some minor adjustments. Some of these issues were raised during a recent review and workshop held by the U.S. Geological Survey (USGS). Others are related to our on-going development and tasks that need to be completed prior to publishing the model. These issues include: (1) the use of worldwide versus western North American data, (2) the impact of surface versus buried rupture for strike-slip and normal faults, (3) hanging-wall effects for normal faults, (4) extrapolating to 10-sec period, and (5) smoothing regression coefficients.

### **Data Selection**

The NGA database includes strong-motion recordings generally intended to represent free-field conditions (i.e., large buildings were excluded). However, we applied additional criteria for deciding whether an earthquake or recording should be used. For example, an earthquake was used only if the following applied: (1) it occurred within the shallow continental lithosphere, (2) it was in a region considered to be tectonically active, (3) it had enough recordings to establish a reasonable source term, and (4) it had generally reliable source parameters. A recording was used only if the following applied: (1) it was at or near ground level, (2) it had negligible structural interaction effects, and (3) it had generally reliable site parameters.

An earthquake was considered to be poorly recorded and excluded from our database if it met the following criteria: (1)  $M < 5.0$  and  $N < 5$ , (2)  $5.0 \leq M < 6.0$  and  $N < 3$ , and (3)  $6.0 \leq M < 7.0$ ,  $r_{rup} > 60$  km and  $N < 2$ , where  $M$  is moment magnitude and  $N$  is the number of recordings. Note that singly recorded earthquakes with  $M \geq 7$  and  $r_{rup} \leq 60$  km were retained because of their importance in constraining near-source ground motion. Specific details regarding how these general criteria were implemented to select the recordings and metadata used in the regression analysis will be documented in a PEER report at the end of the project. The selected database includes over 1500 horizontal recordings from more than 60 earthquakes ranging in magnitude from  $M$  4.2–7.9 and ranging in distance from  $r_{rup} = 0$ –200 km.

### **Regression Analyses**

The regression analyses were performed in two stages (i.e., the two-step regression described by Boore et al. 1993, except that each step used nonlinear regression). In Stage 1, all of those functions involving individual recordings (so-called site or intra-event terms) were fit by the method of nonlinear least squares, in which each earthquake was constrained to have a zero mean residual by assigning it a source term. These functions included Eq. 3 and Eqs. 6–11 in the model presented in the next section. In Stage 2, all of those functions involving the earthquake (so-called source or inter-event terms) from Stage 1 were fit using the method of weighted nonlinear least squares, where each inter-event (source) term was assigned a weight that was inversely proportional to its variance from Stage 1. These functions included Eq. 2 and Eqs. 4–5 in the model presented in the next section. This two-step analysis allowed us to decouple the

intra-event terms from the inter-event terms, which made the regression analysis much more stable and allowed us to independently evaluate and model ground-motion scaling effects at large magnitudes. At the time this paper was written, we had explored the use of random effects regression analysis and have found it to give very similar results as our two-step analysis. As a result, in the final model we will likely use random effects to derive the model coefficients.

### Selection of Functional Forms

We developed the functional forms used in the ground motion relation from classical data exploration techniques including analysis of residuals. Candidate functional forms were developed through numerous iterations to capture the observed trends in the recorded ground-motion data. The final forms include equations developed by ourselves, those taken from the literature, those derived from theoretical studies, and those proposed by the other Developer Teams. We selected the final functional forms based on the following criteria: (1) their simplicity, although this was not an overriding factor, (2) their seismological bases, (3) their unbiased residuals, and (4) their ability to be extrapolated to parameter values important to engineering applications, especially for probabilistic seismic hazard analysis (PSHA). Criterion 4 was the most difficult to meet, because the data did not always allow the functional forms to be developed empirically. In such cases, theoretical constraints were used to define these functional forms based on supporting studies conducted as part of the NGA Project.

The general functional form of the ground motion relation is given by the equation

$$\ln Y = f_1(M) + f_2(R) + f_3(F) + f_4(HW) + f_5(S) + f_6(D) + \varepsilon \quad (1)$$

where  $f_i$  are functions denoting the scaling of ground motion in terms of magnitude ( $M$ ), source-to-site distance ( $R$ ), style of faulting ( $F$ ), hanging-wall effects ( $HW$ ), shallow site conditions ( $S$ ), and sediment or basin depth ( $D$ ); and where each function is defined as follows:

for the function involving magnitude,

$$f_1(M) = \begin{cases} c_0 + c_1M & M \leq 5.5 \\ c_0 + c_1M + c_2(M - 5.5) & 5.5 < M \leq 6.5 \\ c_0 + c_1M + c_2(M - 5.5) + c_3(M - 6.5) & M > 6.5 \end{cases} \quad (2)$$

for the function involving source-to-site distance,

$$f_2(R) = (c_4 + c_5M) \ln \left( \sqrt{r_{rup}^2 + c_6^2} \right) \quad (3)$$

for the function involving style of faulting,

$$f_3(F) = c_7 F_{RV} f_F(H) + c_8 F_N \quad (4)$$

$$f_F(H) = \begin{cases} H & H < 1 \\ 1 & H \geq 1 \end{cases} \quad (5)$$

for the function involving hanging-wall effects,

$$f_4(HW) = c_9 F_{RV} f_{HW}(R) f_{HW}(M) f_{HW}(H) \quad (6)$$

$$f_{HW}(R) = \begin{cases} 1 & r_{jb} = 0 \\ 1 - (r_{jb} / r_{rup}) & r_{jb} > 0 \end{cases} \quad (7)$$

$$f_{HW}(M) = \begin{cases} 0 & M \leq 6.0 \\ 2(M - 6.0) & 6.0 < M < 6.5 \\ 1 & M \geq 6.5 \end{cases} \quad (8)$$

$$f_{HW}(H) = \begin{cases} 0 & H \geq 20 \\ 1 - (H / 20) & H < 20 \end{cases} \quad (9)$$

for the function involving linear and nonlinear shallow site conditions,

$$f_5(S) = \begin{cases} c_{10} \ln\left(\frac{V_{s30}}{k_1}\right) + k_2 \left\{ \ln\left[PGA_r + c\left(\frac{V_{s30}}{k_1}\right)^n\right] - \ln[PGA_r + c] \right\} & V_{s30} < k_1 \\ (c_{10} + k_2 n) \ln\left(\frac{V_{s30}}{k_1}\right) & V_{s30} \geq k_1 \end{cases} \quad (10)$$

and for the function involving shallow-sediment depth and basin effects,

$$f_6(D) = \begin{cases} c_{11}(D - 1) & D < 1 \\ 0 & 1 \leq D \leq 3 \\ c_{12} \left\{ k_3 [0.0000454 - \exp(-3.33D)] + k_4 [0.472 - \exp(-0.25D)] \right\} & D > 3 \end{cases} \quad (11)$$

In the above equations,  $Y$  is the geometric mean of the two horizontal components of peak ground acceleration (PGA,  $g$ ), peak ground velocity (PGV, cm/sec), or 5%-damped pseudo-absolute acceleration response spectra (SA,  $g$ );  $M$  is moment magnitude;  $r_{rup}$  is closest distance to coseismic rupture in kilometers;  $r_{jb}$  is closest distance to the surface projection of coseismic rupture (so-called Joyner-Boore distance) in kilometers;  $F_{RV} = 1$  for reverse and reverse-oblique faulting ( $30^\circ < \text{rake} < 150^\circ$ ) and 0 otherwise, where rake is the average angle measured in the plane of rupture between the strike direction and the slip vector (e.g., Lay and Wallace 1995);  $F_N = 1$  for normal and normal-oblique faulting ( $-150^\circ < \text{rake} < -30^\circ$ ) and 0 otherwise;  $H$  is the depth to the top of coseismic rupture in kilometers;  $V_{s30}$  is the average shear-wave velocity in the

top 30 m in meters per second;  $PGA_r$  is the reference value of PGA on rock with  $V_{s30} = 1100$  m/sec;  $D$  is the depth to the 2.5 km/sec shear-wave velocity horizon (so-called sediment or basin depth) in kilometers;  $n$  and  $c$  are period-independent theoretically constrained model coefficients;  $k_i$  are period-dependent theoretically constrained model coefficients;  $c_i$  are empirically derived model coefficients; and  $\varepsilon$  is a random error term with zero mean and standard deviation given by the equation

$$\sigma_{\ln Y} = \sqrt{\sigma^2 + \tau^2} \quad (12)$$

where  $\sigma$  is the intra-event (within-earthquake) standard deviation from Stage 1 and  $\tau$  is the inter-event (between-earthquake) standard deviation from Stage 2.

### Bases for Functional Forms

The trilinear magnitude-scaling term in Eq. 2 was derived from both an analysis of residuals and theoretical considerations. It models the observed decrease in the amount of magnitude scaling above  $M$  6.5 that was identified in the Stage 2 regression analysis. This behavior, which had been noted in previous studies but not considered credible, became very evident in some well-recorded recent large-magnitude earthquakes in Alaska, California, Turkey and Taiwan. In fact, at the time this paper was written, the regression analysis was producing a slight tendency for over-saturation of short-period ground motion at large magnitudes and short distances. Although some seismologists believe that such over-saturation in short-period ground motion is possible for very large earthquakes, we have found this behavior to be statistically significant. Therefore, in the final model it is likely that we will constrain Eq. 2 so that over-saturation does not occur. Other functional forms were either found to be too difficult to constrain empirically (e.g., the hyperbolic tangent function used by Campbell 1997 or the magnitude-dependent pseudo-distance term used by Campbell and Bozorgnia 2003) or could not be reliably extrapolated to magnitudes as large as  $M$  8.5 (e.g., the quadratic function used by Boore et al. 1997) as required by the NGA Project. For example, in our previous model (Campbell and Bozorgnia 2003), we had to force magnitude saturation in order to prevent over-saturation and to stabilize the nonlinear regression analysis.

The distance-scaling term in Eq. 3 is similar to that used by Abrahamson and Silva (1997). Our previous model (Campbell and Bozorgnia 2003), which was developed for distances of 60 km and less but often used at larger distances, assumed a constant rate of attenuation with magnitude. Since the NGA Project required that the ground motion relations be valid to distances of 200 km, we found it was important to include magnitude-dependent distance scaling in our model in order to extend it to such large distances. The magnitude-dependent distance scaling predicted by Eq. 3 approximates the effects of anelastic attenuation, at least out to the maximum distance of 200 km required by the NGA Project, which Campbell (1997) found to be magnitude-dependent. We also preferred the way that the Abrahamson and Silva functional form transferred the magnitude-dependent distance scaling term from inside the square-root term of Eq. 3, where it served as a pseudo-depth term, to outside the square-root term, where it serves as a pseudo-geometric attenuation term. This shift made the nonlinear regression analysis much more stable.

The style-of-faulting term in Eqs. 4 and 5 was derived from an analysis of residuals. It introduces a new parameter, depth to the top of coseismic rupture ( $H$ ), that indicates whether or not coseismic rupture extends to the surface. This new parameter was found to be most significant at short periods for reverse faulting, although its impact on other types of faulting is still being evaluated. Ground motion was found to be significantly higher for reverse faults when rupture did not break to the surface (i.e., when  $H > 1.0$  km), no matter whether this rupture was on a blind thrust or on a fault with historical or paleoseismic surface rupture. When rupture broke to the surface, ground motion for reverse faults was found to be comparable to that for strike-slip faults. This effect is linearly decreased to zero from depths of 1.0 to 0 km to provide a smooth transition from buried to surface faulting. This transition depth is somewhat arbitrary and was selected so that those faults assigned a depth to the top of rupture of 1.0 km in the 2002 national seismic hazard source model (Frankel et al. 2002) would be treated as a buried fault. Some strike-slip earthquakes with partial or weak surface expression also appeared to have higher-than-average ground motion (e.g., 1995 Kobe, Japan), but additional studies will be required to determine if this is predictable. We found a weak, but significant, trend of increasing ground motion with dip for both reverse and strike-slip faults, but we were not convinced that this trend could be seismologically justified after discussing it with several earth scientists. Therefore, we did not include dip as a parameter at this time, but we will reconsider it in the future when there is more scientific consensus. The coefficient for normal faulting was found to be only marginally significant at short periods. It has been retained at this time because of its potential, but as yet undetermined, significance at longer periods.

Like the style-of-faulting term, the hanging-wall term in Eqs. 6–9 was derived from an analysis of residuals. The functional form for Eq. 7, the term that involves both  $r_{rup}$  and  $r_{jb}$ , was suggested by the Chiou-Youngs Team. We had first proposed a somewhat more complicated functional form that had similar behavior for surface-rupturing earthquakes. However, we switched to the Chiou-Youngs functional form because of its added advantage of smearing out hanging-wall effects over the top edge of a buried rupture, which has been suggested from observations of overturned rocks and transformers near the White Wolf fault, source of 1952 Kern County earthquake, by Brune et al. (2004). We included Eqs. 8 and 9 to phase out hanging-wall effects at small magnitudes and large depths, where the residuals suggest that the effects are negligible or not resolvable from the data.

The linear part of the shallow site conditions term ( $V_{s30} \geq k_1$ ) in Eq. 10 is similar to that originally proposed by Boore et al. (1994) and Borchardt (1994) and later adopted by Boore et al. (1997) and Choi and Stewart (2005). The nonlinear part of this term ( $V_{s30} < k_1$ ) was constrained from theoretical studies conducted as part of the NGA Project (Walling and Abrahamson 2006), since the empirical data were insufficient to constrain the complex nonlinear behavior of the softer soils. After including a linear site term, the resulting residuals clearly indicated the presence of nonlinear behavior of PGA and SA at short periods, but these residuals when plotted against  $PGA_r$  could not be used to determine how this complex behavior varied with  $V_{s30}$ ,  $PGA_r$ , and period. The linear behavior of this model was determined from regression analysis after constraining the nonlinear term to that proposed by Walling and Abrahamson (2006). These authors developed two sets of nonlinear model coefficients based on the site-response simulations of Silva (2005). One set used dynamic soil properties (strain-dependent

shear modulus reduction and damping curves) developed by EPRI (1993), referred to as the EPRI curves, and the other set used dynamic soil properties appropriate for the Peninsular Range, referred to as the PEN curves. Neither our residuals nor the empirical site factors compiled by Power et al. (2004) could distinguish between these two alternatives. The EPRI curves predicted a greater degree of soil nonlinearity in our model than the PEN curves, resulting in relatively higher amplification of short-period ground motion at low values of  $PGA_r$  and relatively greater de-amplification of this ground motion at high values of  $PGA_r$ . We chose to use the results from the PEN curves after Walt Silva (personal communication 2005) suggested that they were probably appropriate for a broader class of sites, and after we found that the intra-event standard deviation was slightly lower (although this was not statistically significant) than for the EPRI curves.

The sediment-depth term in Eq. 11 has two parts: (1) a term to model basin effects for  $D > 3.0$  km and (2) a term to model the effects of shallow sediments for  $D < 1.0$  km, both of which are significant only at long periods. We modeled the depth and period dependence of the basin-effects term with a theoretical model developed by Day et al. (2005) from simulations of the 3D response of the Los Angeles, San Gabriel, and San Fernando basins in southern California, which they conducted for the NGA Project. At our request, Day (2005) extended this model to include the depth to the 2.5 km/sec shear-wave velocity horizon. After including the shallow site conditions term in Eq. 10, the resulting residuals clearly indicated a strong positive trend with  $D$  and period similar to that found by Day (2005) and Day et al. (2005) for  $D > 3.0$  km. However, these authors found that ground motion also scaled strongly with  $D$  between depths of 1.0 and 3.0 km, whereas we did not find any trend in the residuals in this depth range. This effect is apparently accounted for by other parameters in our model (most likely  $V_{s30}$ ). For example, 3.0 km is the depth below which  $D$  and  $V_{s30}$  become strongly correlated in the NGA database. One possible explanation of this correlation is that the 3D simulations are dominated primarily by 1D effects below 3.0 km, which are adequately modeled by  $V_{s30}$ . We calibrated Day's basin-effects model by putting an empirical coefficient in front of his theoretical functional form. We believe that the observed decrease in long-period ground motion at shallow sediment depths ( $D < 1.0$  km) might be a result of the sediment cover being too thin to fully amplify this motion or compensation for a potential over-amplification of ground motion predicted by the shallow site conditions term in Eq. 10 at such shallow depths.

## **Bases for Model Parameters**

The selection of model parameters was tightly linked with the selection of functional forms. The NGA database contains dozens of parameters from which we could choose. We started by selecting parameters that had been found to be important from past studies or by other Developer Teams. After selecting from among those parameters, we evaluated additional parameters from an analysis of residuals. The bases for many of the parameters that were selected are given in the previous section. In this section, we provide further discussion of why we selected some parameters and rejected others.

At first we intended to evaluate all three distance measures in order to select which one might be best. However, the Campbell distance measure ( $r_{seis}$ ), which had been used in our previous model (Campbell and Bozorgnia 2003), was not available for many earthquakes until

late in the NGA Project. Instead, we selected rupture distance ( $r_{rup}$ ) as our preferred distance measure with the intent that we would evaluate the other distance measures at a latter date. However, because of the time-consuming process of finding appropriate functional forms and evaluating the relatively large number of parameters that were provided in the NGA database, we have not as yet had an opportunity to evaluate these other distance measures.

We evaluated all three of the sediment-depth parameters that were provided in the NGA database before selecting  $D$ . These parameters were the depths to the 1.0, 1.5 and 2.5 km/sec shear-wave velocity horizon, referred to as  $Z_{10}$ ,  $Z_{15}$  and  $Z_{25}$ , respectively. We found that  $Z_{10}$  showed the least correlation with both the shallow and deep residual trends that were clearly visible for the other sediment-depth parameters.  $Z_{15}$  and  $Z_{25}$  showed equally good correlation with the deep sediment-depth residuals, but  $Z_{25}$  clearly had the strongest correlation with the shallow sediment-depth residuals. As a result, we selected  $Z_{25}$  as the best overall depth to represent our sediment-depth parameter ( $D$ ).

We spent the greatest amount of time exploring parameters that could explain and model the reduced ground-motion scaling with magnitude that we observed for magnitudes above  $M$  6.5. This scaling is critical because it determines how the model extrapolates to the larger magnitudes of greatest interest in engineering. We plotted the inter-event (Stage 2) residuals against several source and fault parameters, including geologic slip rate, static stress drop, rupture area, coseismic surface rupture, focal depth, asperity depth, amount of shallow moment release, and aspect ratio, among others. Besides coseismic surface rupture, which we included in the model through the parameter  $H$  (discussed earlier), aspect ratio ( $AR$ ) showed the highest correlation with the residuals. All of the other parameters had only a weak correlation.  $AR$  is defined as the ratio of rupture length to rupture width. We first introduced  $AR$  to the other Developer Teams as a possible parameter for quantifying the observed change in ground-motion scaling at large magnitudes based on a recent study by Hanks and Bakun (2002), who found a bilinear relationship between  $M$  and the logarithm of rupture area for strike-slip earthquakes. They found that this bilinear trend began at about  $M$  6.7 and corresponded with the magnitude at which the average coseismic slip becomes proportional to rupture length (so-called L-model scaling). More recently, Halldorsson and Papageorgiou (2005) found that they could not match ground-motion recordings from active tectonic regions using their specific barrier source model without including a parameter that accounted for a significant reduction in ground-motion scaling with magnitude at round  $M$  6.3, which they attributed to a breakdown in self-similarity at large magnitudes. Based on these observations, we tentatively incorporated  $AR$  in our model to explain the observed change in ground-motion scaling at  $AR > 2$ , which approximately corresponds to  $M$  6.5–7.0 for strike-slip faults. However, we later found a discrepancy in the magnitude-dependence of  $AR$  between the NGA database and the 2002 national seismic hazard source model that has temporarily led us to abandon it as a potential source parameter. Once this discrepancy, and its potential bias, is resolved, we will reevaluate using  $AR$  as a parameter in our model, since we believe that it could represent a fundamental property of rupture dynamics.

## Conclusions

Although our NGA ground motion relation is not yet finalized, we believe that it has matured to the point that several significant conclusions can be drawn. One of the most

important conclusions is that several recent large earthquakes in Alaska, California, Turkey and Taiwan have confirmed previous hypotheses that ground motion at close distances from large earthquakes should saturate with magnitude. However, unlike our 2003 model, this saturation is restricted to relatively short periods and large magnitudes. Other significant conclusions from this study are as follows: (1) ground motion from large thrust faults with surface rupture is similar to that from strike-slip faults, (2) ground motion from blind thrust faults and reverse faults with buried rupture is significantly higher than that for strike-slip faults, (3) ground motion from normal faults is only slightly lower than that from strike-slip faults at short periods, although it might become significantly lower at longer periods, (4) nonlinear soil behavior is consistent with that predicted from 1D site-response analyses commonly used in engineering, and (5) there is no significant overall bias between our 2003 and NGA models at two values of  $V_{s30}$  of significance in engineering: 760 m/sec, the NEHRP B-C boundary category used in the USGS national seismic hazard maps, and 270 m/sec, the NEHRP D category used in many site-specific engineering studies. We include Figs. 1–4 as a preview of our NGA ground motion relation.

## References

- Abrahamson, N. A., and W. J. Silva, 1997. Empirical response spectral attenuation relations for shallow crustal earthquakes, *Seism. Res. Lett.* **68**, 94–127.
- Boore, D. M., W. B. Joyner, and T. E. Fumal, 1993. Estimation of response spectra and peak accelerations from western North American earthquakes: An interim report, *U.S. Geol. Surv. Open-File Rept. 93-509*.
- Boore, D. M., W. B. Joyner, and T. E. Fumal, 1994. Estimation of response spectra and peak accelerations from western North American earthquakes: An interim report, Part 2, *U.S. Geol. Surv. Open-File Rept. 94-127*.
- Boore, D. M., W. B. Joyner, and T. E. Fumal, 1997. Equations for estimating horizontal response spectra and peak acceleration from western North American earthquakes: A summary of recent work, *Seism. Res. Lett.* **68**, 128–153.
- Borcherdt, R. D., 1994. Estimates of site-dependent response spectra for design (methodology and justification), *Earthquake Spectra* **10**, 617–653.
- Brune, J. N., A. Anooshehpour, B. Shi, and Y. Zeng, 2004. Precarious rock and overturned transformer evidence for ground shaking in the  $M_s$  7.7 Kern County earthquake: An analog for disastrous shaking from a major thrust fault in the Los Angeles basin, *Bull. Seism. Soc. Am.* **94**, 1993–2003.
- Campbell, K. W., 1997. Empirical near-source attenuation relationships for horizontal and vertical components of peak ground acceleration, peak ground velocity, and pseudo-absolute acceleration response spectra, *Seism. Res. Lett.* **68**, 154–179.
- Campbell, K. W., and Y. Bozorgnia, 2003. Updated near-source ground motion (attenuation) relations for the horizontal and vertical components of peak ground acceleration and acceleration response spectra, *Bull. Seism. Soc. Am.* **93**, 314–331.
- Choi, Y., and J. P. Stewart, 2005. Nonlinear site amplification as function of 30 m shear wave velocity, *Earthquake Spectra* **21**, 1–30.
- Day, S., 2005. 3D ground motion simulation in basins: Supplemental model for the depth to the 2.5 km/sec shear-wave velocity horizon, written communication.
- Day, S., J. Bielak, D. Dreger, S. Larsen, R. Graves, A. Pitarka, and K. B. Olsen, 2005. 3D ground motion simulation in basins, *Project No. IA03*, Pacific Earthquake Engineering Research Center, Richmond, CA.
- EPRI, 1993. Methods and guidelines for estimating earthquake ground motion in eastern North America,

in Guidelines for Determining Design Basis Ground Motions, *Rept. No. EPRI TR-102293*, Vol. 1, Electric Power Research Institute, Palo Alto, CA.

Frankel, A. D., M. D. Petersen, C. S. Mueller, K. M. Haller, R. L. Wheeler, E. V. Leyendecker, R. L. Wesson, S. C. Harmsen, C. H. Cramer, D. M. Perkins, and K. S. Rukstales, 2002. Documentation for the 2002 update of the national seismic hazard maps, *U.S. Geol. Surv. Open-File Rept. 02-420*.

Halldorsson, B., and A. S. Papageorgiou, 2005. Calibration of the specific barrier model to earthquakes of different tectonic regions, *Bull. Seism. Soc. Am.* **95**, 1276–1300.

Hanks, T. C., and W. H. Bakun, 2002. A bilinear source-scaling model for  $M$ -log  $A$  observations of continental earthquakes, *Bull. Seism. Soc. Am.* **92**, 1841–1846.

Lay, T., and T. C. Wallace, 1995. *Modern Global Seismology*, Academic Press, San Diego, CA.

Power, M., R. Borchardt, and J. Stewart, 2004. Site amplification factors from empirical studies, *Report of NGA Working Group No. 5*, Pacific Earthquake Engineering Research Center, Richmond, CA.

Silva, W. J., 2005. Site response simulations for the NGA project, *Draft report*, Pacific Earthquake Engineering Research Center, Richmond, CA.

Walling, M., and N. Abrahamson, 2006. Non-linear soil response model, this volume.

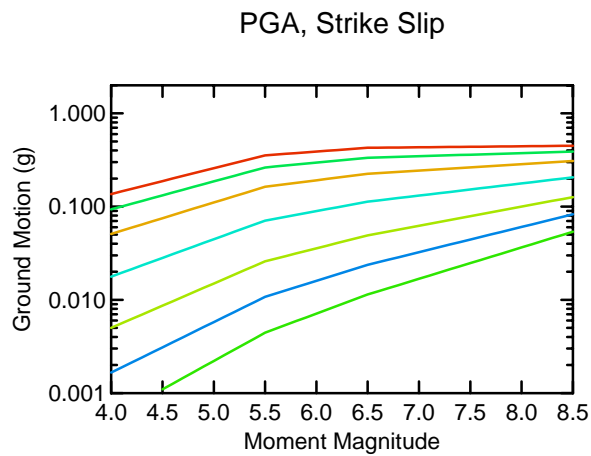


Figure 1. PGA versus  $M$  for  $r_{rup} = 0$ –200 km.

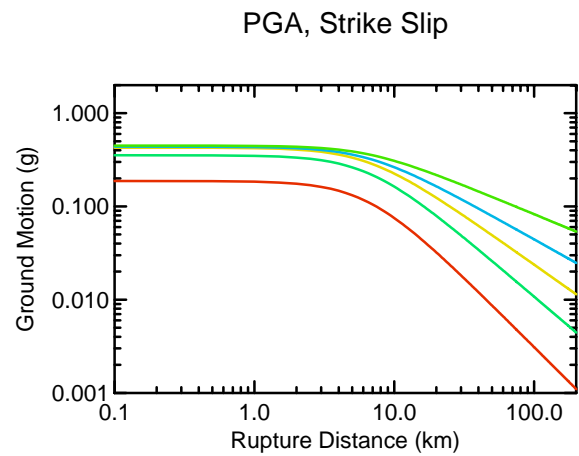


Figure 2. PGA versus  $r_{rup}$  for  $M = 4.5$ –8.5.

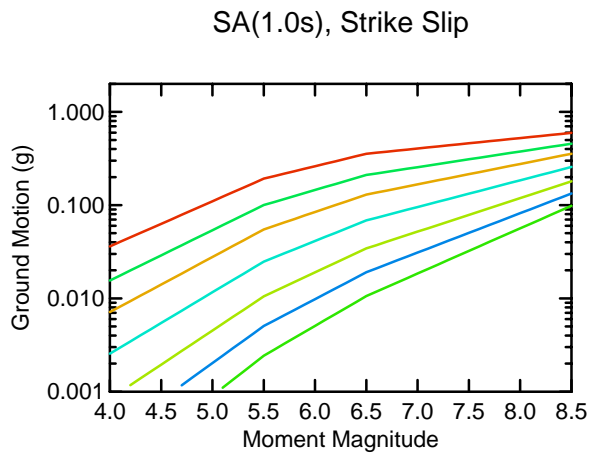


Figure 3. SA(1.0s) versus  $M$  for  $r_{rup} = 0$ –200 km.

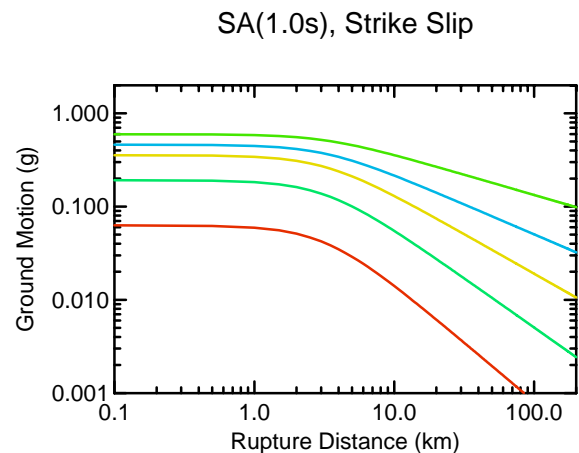


Figure 4. SA(1.0s) versus  $r_{rup}$  for  $M = 4.5$ –8.5.